Available online at www.sciencedirect.com
ScienceDirect
Food Chemistry 105 (2007) 667–674
Food Chemistry
www.elsevier.com/locate/foodchem

Analytical, Nutritional and Clinical Methods

Fast, clean, low-cost screening of cadmium and lead in the mussel *Mytilus galloprovincialis* Lmk. by visible spectroscopy and partial least squares regression

Rafael Font [a,*], Dinoraz Vélez [b], Mercedes del Río-Celestino [c], Antonio de Haro-Bailón [a], Rosa Montoro [b]

[a] *Instituto de Agricultura Sostenible (CSIC), Alameda del Obispo s/n, 14080 Córdoba, Spain*
[b] *Instituto de Agroquímica y Tecnología de Alimentos (CSIC), Apartado 73, 46100 Burjassot, Valencia, Spain*
[c] *IFAPA-CICE, CIFA-Córdoba (Junta de Andalucía), Alameda del Obispo s/n, 14080 Córdoba, Spain*

Received 7 July 2006; received in revised form 25 December 2006; accepted 27 December 2006

Abstract

The potential of visible (VIS) spectroscopy for screening cadmium and lead contents in the mussel *Mytilus galloprovincialis* Lmk. was assessed. The spectra of the samples were recorded (400–700 nm). The Cd and Pb contents were determined by graphite furnace atomic absorption spectroscopy, and were regressed against different spectral transformations by modified partial least square (PLSm) regression. Coefficients of determination in the cross-validation (Cd = 0.95; Pb = 0.77) were indicative of equations with excellent and good quantitative information, respectively. The standard deviation to standard error of cross-validation ratio (Cd = 4.43; Pb = 2.10) showed sufficient predictive accuracy for the equations to be used for screening purposes. PLSm loading plots corresponding to the first terms of the equations showed that chromophores influenced them significantly. This pioneering use of the VIS spectrum to predict Cd and Pb in mussels represents an important saving in time and cost of analysis in comparison to other methods.

Keywords: Least squares regression; Lead; Cadmium; *Mytilus galloprovincialis*

1. Introduction

Marine mollusks are widely distributed all over the world and are intensively studied because most of them are commercially valuable species, being easy to cultivate or collect in coastal areas. They are also generally known to be very useful organisms for monitoring pollution by trace elements. Among mollusks, the soft tissues of *Mytilus* spp. mussels have been studied extensively from both food safety (Behrens Yamada & Peters, 1988; Pérez Camacho, González, & Fuentes, 1991) and ecotoxicological (Goldberg & Bertine, 2000; Gorinstein et al., 2003) points of view because of their potential for accumulating trace elements at higher concentrations than those found in the surrounding seawater, acting as a vector of contamination in the food chain. Among the different species of mussels found in Europe, *Mytilus galloprovincialis* Lmk. has been reported as the only species of the genus which is present in both the Atlantic and the Mediterranean coastal areas of the Iberian Peninsula (Sanjuan, Quesada, Zapata, & Alvarez, 1990). This species represents an important resource for fishery in Spain, with a declared mean annual production in Galicia (which represents 95% of total mussel production in Spain) of approximately 260×10^6 kg in raft culture in 2005. The remaining 5% is produced in Catalonia, the Valencian Community and the Balearic Islands. This makes Spain the second producer of mussels in the world, after China. Moreover, Spanish mussel exports are increasing quickly, mainly in Europe, where a country such as Belgium imports over 12×10^3 kg of *M. galloprovincialis* a day.

* Corresponding author. Fax: +34 957499252.
E-mail address: font@cica.es (R. Font).

0308-8146/$ - see front matter © 2007 Elsevier Ltd. All rights reserved.
doi:10.1016/j.foodchem.2006.12.055

This has made the control of trace elements in mussels a subject of great concern for the Spanish and European authorities, leading the Commission of the European Communities and the Scientific Committee for Food jointly to establish criteria for performing trace element determinations, and also to legislate on the maximum contents allowed for certain contaminants in foodstuffs. In bivalve mollusks, limits have been established for Cd (1 mg kg^{-1} wet weight) and Pb (1.5 mg kg^{-1} wet weight) (Official Journal of the European Communities, 2001). Cd and Pb can be considered xenobiotic elements with a high tendency to bioaccumulation, although distributed in the marine environment at low concentrations. Their adverse effects on human health include anemia, abortions, renal and cerebral damage, hypertension, neurological alterations, gastrointestinal perturbations, and cancer, among others (Concon, 1988).

The need to perform numerous Cd and Pb tests to assess contamination in mussels intended for internal consumption or for export trade imposes a heavy burden of labor input and expenditure on regional and central Spanish administrations. Contamination is assessed by making a high number of analyses using standard methods (atomic absorption spectrometry and stripping voltammetry). Although these techniques for elemental analysis usually offer high levels of accuracy and precision, they also have some disadvantages, such as the use of hazardous chemicals, high labor input and costs, and delays in obtaining results, all of which affect both the availability of data and the taking of swift decisions. These factors have led to a search for alternative analytical techniques to solve the problems associated with the conventional ones.

In recent decades the development of equipment featuring improved electronic and optical components, the advent of computers capable of efficiently processing the information contained in spectra, and the development of powerful chemometric applications have facilitated the expansion of spectroscopic techniques for elemental analysis in an increasing number of fields, allowing efficient management of spectral and chemical data. Among these techniques, high resolution spark source mass spectroscopy (Ball, Barber, & Vossen, 1975), X-ray energy spectroscopy (Stump, Kearney, D'Auria, & Popham, 1979), Fourier transform spectroscopy (Feo & Aller, 2001; Hren, Mink, & Balázs, 2002) and near-infrared spectroscopy (NIRS) (Font, Del Río-Celestino, Vélez, De Haro-Bailón, & Montoro, 2004) have been applied to this area. So far, however, no studies have been reported that use only the information provided by the visible (VIS) spectral segment to assess trace element concentration in biological or non-biological matrices, which is a novel, practical application with benefits over other spectroscopic techniques. The benefits include lower cost and easier management of equipment compared with the methods mentioned previously, making it an accessible technique for most laboratories.

The present study shows, for the first time, the potential of VIS spectroscopy combined with partial least squares (PLS) regression for fast, cost-effective screening of Cd and Pb concentrations in the species *M. galloprovincialis*. A possible explanation for the technique's success in assessing concentrations of these two elements in mussel is given, based on the establishment of indirect correlations that relate the concentration of the elements in the animal tissues with light absorption by chromophores.

2. Materials and methods

2.1. Equipment and software

Visible spectra were recorded on a VIS–NIR spectrometer model 6500 (Foss-NIRSystems, Inc., Silver Spring, MD, USA) in reflectance mode equipped with a transport module. The monochromator 6500 consists of a tungsten bulb and a rapid scanning holographic grating with detectors positioned for transmission or reflectance measurements. To produce a reflectance spectrum, a ceramic standard is placed in the radiant beam, and the diffusely reflected energy is measured at each wavelength. The actual absorbance of the ceramic is very consistent across wavelengths. In this work, each spectrum was recorded once from each sample, and was obtained as an average of 32 scans over the sample, plus 16 scans over the ceramic standard before and after scanning the sample. The ceramic and the sample spectra are used to generate the final log ($1/R$, where R is reflectance) spectrum. The total analysis time per sample was 1.50 min.

Mathematical transformations of the spectra and regressions performed on the spectral and laboratory data were obtained by using the GLOBAL v. 1.50 chemometric application (WINISI II, Infrasoft International, LLC, Port Matilda, PA, USA).

2.2. Instruments

Determinations of Cd and Pb were performed by graphite furnace atomic absorption spectroscopy (GFAAS) with longitudinal AC Zeeman (AAnalyst 600 Perkin Elmer, Spain), equipped with a transversely heated graphite atomizer and a built-in, fully computer-controlled AS-800 autosampler (Perkin Elmer). Pyrolytic graphite-coated tubes with an inserted L'vov platform were used. A domestic microwave oven (model Optiquick DUO, Moulinex, Spain), with a maximum power of 900 W was employed for sample digestion.

2.3. Sampling

The mussels used for the study were grown in raft culture at three sites on the Iberian Peninsula; one on the Atlantic coast (Autonomous Community of Galicia, L1), and two on the Mediterranean coast (Autonomous Communities of Catalonia, L2, and Valencia, L3). These

sampling sites represent the main mussel production areas in Spain. The mussels were collected in July, 2004 and were mature animals. A total of 51 specimens (16 from L1, 16 from L2, and 19 from L3) was captured initially for the study, but one of them (from L2) was later discarded. Only the soft tissues of the mollusk were used in the study. The soft tissues were cleaned, frozen at −20 °C, freeze-dried, and then crushed to a fine powder in a mill. The resulting powder was stored at 4 °C until analysis.

2.4. Cadmium and lead determination

Cd and Pb determinations were carried out following the method reported by Almela et al. (2002). Commercial standard solutions (1000 mg L^{-1}) of Pb and Cd were used (Merck, Merck Farma y Química, S.A., Barcelona, Spain). Deionized water (18.2 MΩ cm) was used to prepare the reagents and standards. The sample (0.20 g) was placed in a high-pressure poly(tetrafluoroethylene) vessel, and 2 mL of 65% HNO_3 and 1 mL of 35% H_2O_2 were added. The vessel was sealed with a screw cap and placed inside the microwave oven. Samples were irradiated at a 700 W power setting for 3 cycles of 1 min. After digestion, the solutions were cooled, filtered, and diluted with water to a final volume of 25 mL. The furnace program [temperature (°C)/ramp time (s)/hold time (s)] employed for Cd determination was: drying 90 °C/10 s/20 s; 120 °C/10 s/20 s; 130 °C/5 s/40 s; 300 °C/5 s/5 s; pyrolysis: 500 °C/10 s/20 s; cooling: 20 °C/10 s/20 s; atomization: 1400 °C/0 s/5 s; cleaning: 2450 °C/1 s/5 s. For the determination of Pb, the same furnace program was used, with the exception of the temperatures for pyrolysis (850 °C) and atomization (1600 °C). The matrix modifier used for determining the two metals was a mixture of 0.067 mg $H_2PO_4NH_4$ and 0.003 mg $Mg(NO_3)_2$ in 1% HNO_3 (v/v). The quantification of Pb and Cd was performed using calibration curves of the corresponding standards. Triplicate analyses were performed for each sample. The limit of detection was 0.05 mg kg^{-1} dry weight (dw) for Pb and 0.003 mg kg^{-1} dw for Cd. The accuracy of measurement throughout the experiment was checked by analyzing one certified reference material with each batch of samples: DORM-2 (Dogfish muscle) or TORT-2 (Lobster hepatopancreas), both from the Institute for Environmental Chemistry, National Research Council Canada (NRC, Ottawa, Canada).

2.5. NIRS procedure: recording of spectra

Freeze-dried, ground samples of the mussels collected in L1, L2, and L3, were placed in the sample holder (3 cm diameter, 10 mL volume approximately) until it was full (sample weight ≅3.50 g), and were then scanned. Their spectra were acquired at 2 nm wavelength resolution as $\log 1/R$ (where R is reflectance) over a wavelength range from 400 to 2500 nm (visible plus near-infrared regions), but only the visible segment of the spectrum (from 400 to 700 nm) was considered in this study.

2.6. Pre-treatments of spectral data

The spectra file was checked for spectral outliers [spectra with a standardized distance from the mean(H) > 3 (Mahalanobis distance)], by using principal component analysis (PCA) (Shenk & Westerhaus, 1991). The objective of this procedure was to detect possible samples whose spectra differed significantly from the mean spectrum in the set used to conduct this study.

Raw spectra in the form of $\log 1/R$ were transformed to their first and second-order derivatives, with several combinations of segment (smoothing) and derivative (gap) sizes [i.e., (0, 0, 1, 1; derivative order, segment of the derivative, first smooth, second smooth); (1, 4, 4, 1); (2, 5, 5, 2)] (Shenk & Westerhaus, 1996). In addition to the use of derivatives, standard normal variate and de-trending (SNV-DT) transformations (Barnes, Dhanoa, & Lister, 1989) were used to correct baseline offset due to scattering effects produced by differences in particle size and path length variation among samples.

2.7. Performing regression

To correlate the spectral information (raw optical data or derived spectra) of the samples and Pb and Cd contents determined by the GFAAS method, modified partial least squares (PLSm) was used as a regression method, using different number of wavelengths from 400 to 700 nm for the calculation.

The objective was to perform a linear regression in a new coordinate system with a lower dimensionality than the original space of the independent variables. The PLS factors were determined by the maximum variance of the independent (spectral data) variables and by a maximum correlation with the dependent (chemical) variables. The model obtained used only the most important factors, the noise being encapsulated in the less important factors.

2.8. Cross-validation

The performances of the different calibration equations obtained for Cd and Pb were determined from cross-validation (Martens & Naes, 1989), thus avoiding the bias produced when a low number of samples representing the full range is selected as an external validation set (Shenk & Westerhaus, 1996; Williams & Sobering, 1996).

The statistics coefficient of determination in the cross-validation (R^2_{cval}, Eq. (1)) (Shenk & Westerhaus, 1996) and standard deviation (SD) to standard error of cross-validation (SECV) ratio Eq. (2) (Dunn, Beecher, Batten, & Ciavarella, 2002; Williams & Sobering, 1996) were used as indicators of the performance of the equations

$$R^2_{cval} = \left(\sum_{i=1}^{n}(\hat{y}-\bar{y})^2\right)\left(\sum_{i=1}^{n}(y_i-\bar{y})^2\right)^{-1} \quad (1)$$

where $\hat{y}$ = NIR measured value; $\bar{y}$ = mean "y" value for all samples; y_i = lab reference value for the ith sample

$$\text{SD SECV}^{-1} = \text{SD}\left\langle \left[\left(\sum_{i=1}^{n} (y_i - \hat{y}_i)^2 \right) (n - K - 1)^{-1} \right]^{0.5} \right\rangle^{-1} \quad (2)$$

where y_i = lab reference value for the ith sample; $\hat{y}$ = NIR measured value; n = number of samples, K = number of wavelengths used in an equation; SD = standard deviation.

Those samples showing a "t" value greater than 2.5 and H value greater than 3 were identified in cross-validation as being chemical or spectral outliers, respectively (Shenk & Westerhaus, 1996).

3. Results and discussion

3.1. Cadmium and lead contents in mussel samples

The mussels had Cd contents ranging from 253 (L3) to 1324 (L2) ng g^{-1} of dw (Table 1). Specimens collected at L1 and L2 were found to show the highest Cd contents of the three sampling points, with mean values that did not differ significantly ($p < 0.05$). L3 was the coastal location in which mussels exhibited the lowest Cd contents of all, with a mean value approximately 3.5 times lower than those of L1 and L2.

The Pb contents of the mussel samples ranged from 80 (L2) to 2295 (L3) ng g^{-1} of dw (Table 1). The mussels had mean concentrations of Pb that differed significantly ($p > 0.05$) between the three sampling areas. Specimens collected at L3 showed the highest Pb mean concentration (1697 ng g^{-1} of dw) of the three sampling points, approximately 2.5 and 5 times greater than the contents of samples collected at L1 (685 ng g^{-1} dw), and L2 (353 ng g^{-1} of dw), respectively.

3.2. VIS reflectance spectrum of mussel

Fig. 1 shows the second derivative (2, 5, 5, 2; order of derivative, gap, first smooth, second smooth) averaged reflectance spectrum of mussel populations (freeze-dried, ground soft tissues) from L1, L2, and L3. The main absorption bands shown by the averaged spectra exhibited absorption maxima (λ_{max}) at 476, 506, 554, 604, and 668 nm, determined in second derivative spectra by peaks pointing downward. These bands between 400 and 700 nm are related to light absorption by pigments which dominates the reflectance spectrum at these wavelengths as a consequence of electronic transitions taking place in the photoactive part of the molecule (chromophore).

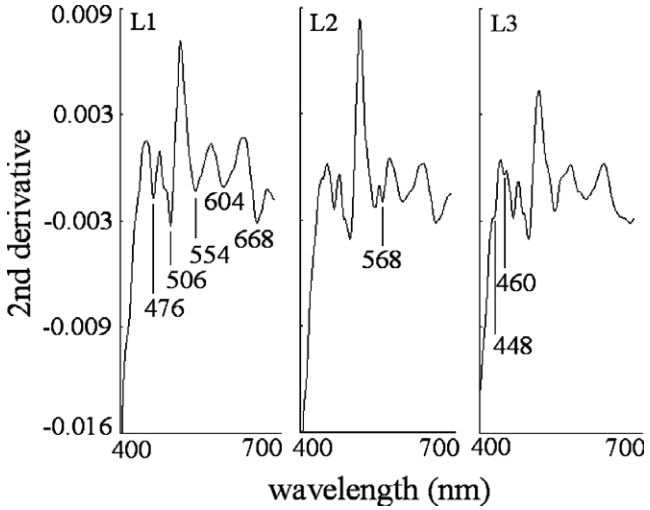

Fig. 1. Average spectra (2, 5, 5, 2) of the freeze-dried mussel samples ($n = 50$) corresponding to locations L1 (Galicia), L2 (Catalonia), and L3 (Valencia) in the range from 400 to 700 nm.

Several carotenoids reported (Partali, Tangen, & Liaaen-Jensen, 1989) in the genus *Mytilus* might be influencing the absorption band at $\lambda_{max} = 476$ nm, which is displayed by spectra from mussels collected at the L1, L2, and L3 sampling locations. They include fucoxanthin (5,6-epoxy-3,3′,5′-trihydroxy-6′,7′-didehydro-5,6,7,8,5′,6′-hexahydro-β,β-caroten-8-one 3′-acetate), alloxanthin [(3*R*, 3′*R*)-7,8,7′, 8′-tetradehydro-β,β-caroten-3,3′-diol], β,β-carotene, crocoxanthin [(3*R*,6′*R*)-7,8-didehydro-β,ε-caroten-3-ol], mytiloxanthin and peridinin [(3*S*,5*R*,6*R*, 3′*S*,5′*R*,6′*S*)-5′,6′-epoxy-3,5,3′-trihydroxy-6,7-didehydro-5,6,5′,6′-tetrahydro-10,11,20-trinor-β,β-caroten-19′,11′-olide 3-acetate]. Most of these carotenoids have been reported in algae belonging to the botanical groups of rhodophyta (β-carotenes), pyrrophyta (peridinin and fucoxanthin), chrysophyta (fucoxanthin), cryptophyta (alloxanthin and crocoxanthin) and phaeophyta (fucoxanthin) (Goodwing & Britton, 1988). In addition, chlorophyll has also been shown to present λ_{max} at around 470 nm in green algae (Britton, 1995).

A weak absorption band at $\lambda_{max} = 460$ nm appears as a specific trait of the spectrum of mussels collected at L3. Two other different carotenoids, echinenona (β,β-caroten-4-one), which is a ketocarotenoid well distributed in cyanobacteria, and pyrroxanthin, have been found to absorb at $\lambda_{max} = 461$ and 459 nm, respectively (Goodwing & Britton, 1988), and might explain the occurrence of that weak absorption band in the L3 population.

Table 1
Mean ± standard deviation and ranges (parentheses) of cadmium and lead contents in the mussel samples

Element	Location 1 (Galicia) $n = 15$	Location 2 (Catalonia) $n = 16$	Location 3 (Valencia) $n = 19$
Cd	1110 ± 125[a] (821–1307)	1154 ± 119[a] (1026–1324)	306 ± 46[b] (253–413)
Pb	685 ± 287[a] (308–1319)	353 ± 289[b] (80–1133)	1697 ± 325[c] (979–2295)

Results expressed as ng g^{-1} of dry weight.

[a] Values followed by the same letter are not significantly different at the 0.05 probability level based on t-tests.

At longer wavelengths, pigment-protein complexes could be the molecules responsible for some traits characterizing the VIS region. For instance, phycoerythrins, a class of phycobiliproteins, have been shown to absorb in a range from 498 to 568 nm; phycocyanins at about 625 nm; and most allophycocyanins absorb maximally around 650 nm, although they can range from 618 to 673 nm.

In the red region of the spectrum, electronic transitions are experienced by the chlorophyll *a*/*b* protein, showing absorption bands located at 652 and 670 nm (Goodwing & Britton, 1988), which match absorptions at 668 nm shown in the spectra of mussels from L1, L2, and L3 (Fig. 1) at the longest wavelengths.

As the soft tissues of the mussel samples used to conduct this work were processed whole, without removing the digestive tract from the carcass and, therefore, the microalgae contained in the digestive tract of the animals at the time of processing, those algae species might explain some of the absorptions shown by the spectra.

3.3. Population structuring and spectral traits characterizing L1, L2, and L3 mussel populations

PCA was carried out on the transformed second-derivative spectra (2, 5, 5, 2; SNV + DT), resulting in 16 principal components (factors) that explained 99% of the total spectral variance. Spectral differences exhibited by the VIS segment of the L1, L2, and L3 mussel populations resulted in spectra (scores) grouped into three clearly separate clusters which corresponded to the three sampling locations considered in this study. In this work, PCA resulted in one mussel sample at L2 being identified as a spectral outlier ($H > 3$), which was eliminated from the study group, as it was not possible to scan the sample again.

The main VIS spectral traits shown by mussels from L1, L2, and L3 which explain the clustering are shown (Fig. 2 L1, L2, and L3). Spectral regions of maximum variability for each mussel population were determined by plotting the standard deviations of the absorbance data (in the form of their second derivative; SNV + DT) against wavelength absorption in the segment from 400 to 700 nm (one absorbance value every 2 nm of wavelength resolution). It was concluded that mussels collected at L2 and L3 (Mediterranean coast) showed SD profiles that were more similar to each other than the profile exhibited by mussels from L1 (Atlantic coast). Maximum differences shown by Atlantic mussels with respect to the Mediterranean ones were lower overall SD values through the entire spectral segment, except at wavelengths related to chlorophyll (Chl) absorption, in which mussels from L1 showed a higher SD value. At shorter wavelengths (from 400 to 500 nm), which are dominated by carotene absorptions (Britton, 1995), mussels from the Mediterranean coast had higher SD values than the Atlantic ones. However, the SD profiles of the mussels from L2 and L3 were very complex, and minor differences were found between them, both at shorter and longer wavelengths.

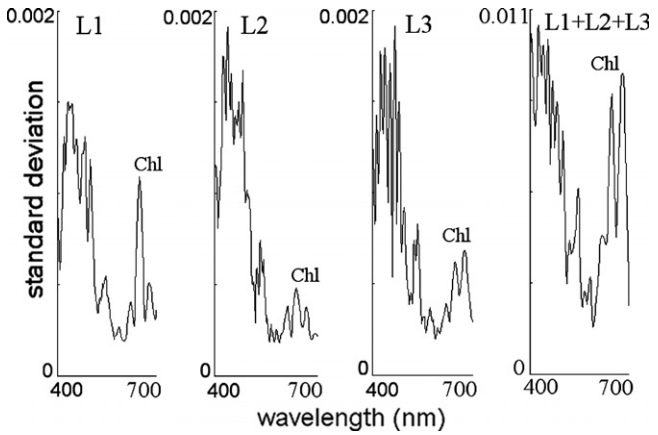

Fig. 2. Standard deviation plots for wavelength absorption (2, 5, 5, 2; SNV + DT) in the range from 400 to 700 nm corresponding to mussel populations L1 (Galicia), L2 (Catalonia), and L3 (Valencia), and also for the three populations jointly (L1 + L2 + L3). Chl: chlorophyll.

It has been reported (Jensen & Sakshaug, 1970) that planktonic blooms could be responsible for the total concentration of carotenoids found in mussel samples, although other factors, such as local differences in food availability (algae species and relative percentage of appearance), could at least partly explain differences in the SD absorbance values shown by mussel populations at L1, L2, and L3. Quantitative and qualitative differences in the pigment profile of soft tissues of mussels belonging to the same species but inhabiting separate coastal zones have been reported on the basis of differences in food availability (Partali et al., 1989). The SD values vs. wavelength shown when the three mussel populations were considered jointly (L1 + L2 + L3) had a different pattern than those displayed by the independent groups (Fig. 2). In addition to the overall increase in the SD values shown, the wavelengths related to Chl absorption (at around 650 and 682 nm) experienced both absolute and relative increases with respect to SD values due to carotene absorptions, as expected.

3.4. Correlation plots for Cd and Pb

Correlation plots for Cd and Pb at L1, L2, and L3 were obtained (Fig. 3) to search for relations between element concentration in the samples and variations in absorptions at specific wavelengths that could possibly be used by PLSm regression to construct the equation factors (Osborne, Fearn, & Hindle, 1993). Correlelograms standardized by using SNV plus DT algorithms are shown in Fig. 3. They represent the correlations shown by the Cd and Pb reference concentrations in the samples vs. absorbance by chromophores at each wavelength and location.

It must be noted that the sign of the plots of L1, L2, and L3 showed an inverse correlation at most wavelengths, which resulted in correlelograms for Cd and Pb showing a mirror-image-like appearance. This must be interpreted

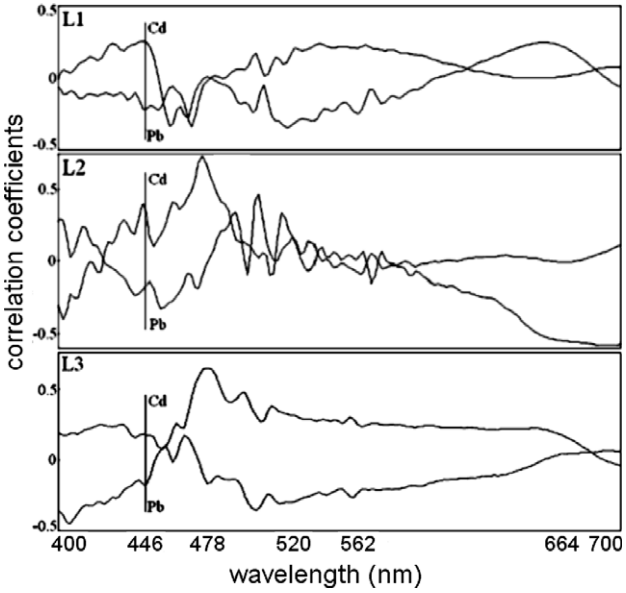

Fig. 3. Correlation plots for cadmium and lead reference values vs. wavelength absorbance by using SNV + DT algorithms, in the range from 400 to 700 nm, corresponding to locations L1 (Galicia), L2 (Catalonia), and L3 (Valencia) ($n = 50$).

in the context of the positive and negative correlations between certain absorbers (chromophores) and the Cd and Pb concentrations, as there were very low correlations between the two elements at each of the three sampling areas ($r_{L1} = 0.03$; $r_{L2} = 0.12$ $r_{L3} = 0.13$).

Some features are worth highlighting in the plots for L1, L2, and L3 (Fig. 3). For instance, the correlation plots for L1 and L3 were similar, sharing overall shapes that were different from the correlation plot of samples collected at L2. For Cd, positive correlations that might be related to carotene and chlorophyll absorptions were found at the shortest VIS wavelengths at L1 and L3, while for mussels from L2 the opposite occurred. Pb showed a pattern of inverse sign to the Cd pattern at those wavelengths. On the other hand, samples from L2 displayed a more complex plot in the segment from 500 to 600 nm than the L1 and L3 populations, in spite of the similar environmental conditions in the Mediterranean coastal area shared by samples from L2 and L3. However, some local maxima were common traits in the correlation plots of samples from L2 and L3, such as the maximum occurring around 478 nm, where most mussel carotenoids have been reported to absorb (Goodwing & Britton, 1988; Partali et al., 1989). At that wavelength, the sign of the L1 correlelogram was the inverse of the correlelogram of the Mediterranean mussels, with Cd and Pb showing a negative correlation with absorbers at around 480 nm.

Any conclusion concerning trace element correlations with absorptions in the VIS reflectance spectrum has to allow for the fact that such observations are based on indirect correlations established with cell chromophores. Trace elements enter mussels mainly through diet, although the byssal threads contain a few binding sites available for scavenging metals from seawater (Coombs & Keller, 1981). One important source of environmental food variability for mussel species appears to be associated with changes in both the concentration and species composition of the phytoplankton community that may result from different change scales, including short-term tide-driven resuspension events (Bayne, 1993). Thus, Cd assimilation by mussels has been reported to be significantly dependent on food composition (Wang & Wong, 2003).

These factors probably determine some of the data presented, and could provide a total or partial explanation of the relation existing between element concentration in the mussel samples and changes in apparent absorption by chromophores.

3.5. Pre-treatment of spectral data and equation performance

Raw spectra ($\log 1/R$) of freeze-dried, ground mussels were transformed to their second derivative (2, 5, 5, 2; SNV plus DT algorithms), which resulted in substantial correction of the baseline shift caused by differences in particle size and path length variations, and yielded the equations for Cd and Pb with the highest predictive ability of the different equations developed. The second derivative has peaks and troughs that correspond to the points of maximum curvature in the raw spectrum, and it has a trough corresponding to each peak in the original. The increase in the complexity of the derivative spectra resulted in a clear separation between peaks that overlap in the raw spectra. In addition, wavelengths every 8 nm were used for calculation in the range from 400 to 700 nm. The use of these mathematical approaches yielded the equations with a higher predictive ability in cross-validation than any other of the various mathematical treatments used.

PLSm regression resulted in a calibration equation for Cd which was modeled with four terms. This is in the range recommended to avoid over-fitting, i.e., one term for each ten samples in the calibration set (Shenk & Westerhaus, 1991). The equation showed a standard error of calibration (SEC) of 52 ng g^{-1} dw and a coefficient of determination in the calibration (R^2_{cal}) of 0.98 (Table 2). The equation was cross-validated, resulting in a SD $SECV^{-1}$ ratio of 4.43 and an R^2_{cal} of 0.95, i.e., 95% of the chemical variance of data was explained by the model in the cross-validation. These statistics characterize the equation as excellent (Dunn et al., 2002) and showing excellent quantitative information (Shenk & Westerhaus, 1996), respectively.

As in the case of Cd, lead was best modeled with the second derivative transformation (2, 5, 5, 2; SNV + DT) of the $1/R$ data prior to calibration. PLSm regression resulted in a calibration equation that had one term and showed a SEC of 299 ng g^{-1} dw and an R^2_{cal} of 0.80 (Table 2). In cross-validation the equation showed a SD $SECV^{-1}$ ratio of 2.10 and an R^2_{cval} of 0.77, which were indicative of equations suitable for screening purposes and good quantitative information, respectively.

Table 2
Calibration and cross-validation statistics for cadmium and lead for the selected equations ($n = 50$)

Element	Calibration					Cross-validation		
	Range	Mean	SD	SEC	R^2_{cal}	SD SECV^{-1}	R^2_{cval}	nt
Cd	253–1307	790	407	52.38	0.98	4.43	0.95	4
Pb	80–2295	947	651	298.96	0.80	2.10	0.77	1

Range = minimum and maximum reference chemistry values in the calibration file (ng g^{-1} of dry weight); SD = standard deviation of the calibration file (ng g^{-1} of dry weight); SEC = standard error of calibration (ng g^{-1} of dry weight); R^2_{cal} = coefficient of determination in the calibration; SD SECV^{-1} = SD to standard error of cross-validation ratio; R^2_{cval} = coefficient of determination in cross-validation; nt = number of terms in the selected equation.

No spectral outliers were identified in cross-validation in the calibrations for Cd and Pb. However, two samples in the calibration for Cd and one sample in the calibration for Pb were found to have t values greater than 2.5, and were identified as chemical outliers. It was decided to keep these samples in the calibration groups for Cd and Pb, once their reference values had been confirmed.

3.6. Partial least squares modified loadings for Cd and Pb equations

The equation selected for Pb was modeled with one term, and this single factor showed a loading plot almost identical to the one for the first factor for the Cd equation, but of inverse sign (Fig. 4). Of the first three factors modeling the Cd equation, the third was the one most closely correlated to the Cd content in the samples, showing that wavelengths 448, 464, 480, 528 and 560 nm strongly influenced this term of the equation (Fig. 4, panel PLSm 3 Cd). These wavelengths were also systematically used in constructing factors 1 (Fig. 4, panel PLSm Cd 1) and 2 (Fig. 4, panel PLSm Cd 2). The first term was also influenced by the red segment of the spectrum, in which absorptions at around 664–688 nm, possibly attributable to absorption by chlorophyll, participated highly in its development.

One can conclude from the PLSm loading plots that spectral regions showing maximum variability as expressed by their SD values (Fig. 2, L1 + L2 + L3), such as the ones at the shortest (blue) and longest wavelengths (red), contributed substantially to the development of the calibration equations for Cd and Pb. For instance, wavelengths 440, 464, 480 and 682 nm, which correspond to local maxima in the SD spectra (Fig. 2), were actively used in the decomposition of the data for the Cd and Pb equations. Moreover, these wavelengths showed high correlation values with Cd and Pb contents (Fig. 3), and in general they matched positive or negative maxima in the correlation plots corresponding to the L1, L2, and L3 populations.

Additional spectral regions actively used in the decomposition, such as those from 520 to 528 nm, and from 550 to 568 nm, were represented by local maxima in the SD plots (Fig. 2, L1 + L2 + L3), and also showed overall high positive or negative correlations with element concentrations (Fig. 3).

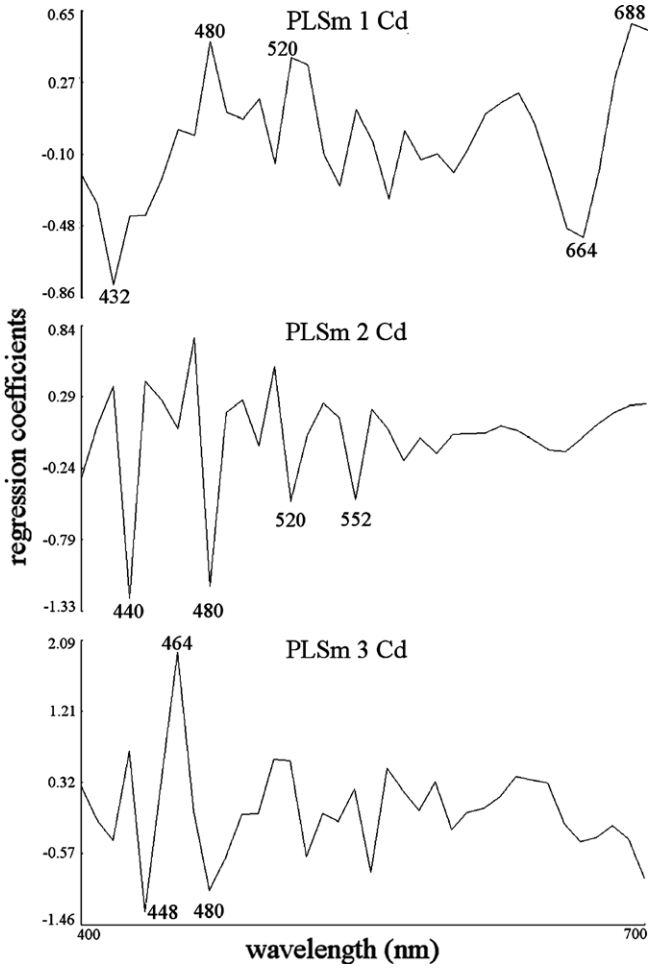

Fig. 4. PLSm loading spectra for cadmium in mussel samples corresponding to the second derivative (2, 5, 5, 2; SNV + DT) equation. From top to bottom, the panels show the regression coefficients corresponding to the first, second, and third terms of the cadmium equation for wavelengths from 400 to 700 nm.

3.7. Use of VIS spectroscopy for metal screening purposes

Prediction results obtained from cross-validation showed for the first time that the VIS region of the spectrum can be used for fast, cost-effective screening of Cd and Pb at low, medium, and high contents in freeze-dried samples of the mussel *M. galloprovincialis*. The Commission of the European Communities and the Scientific Committee for Food have jointly set the maximum permissible

content for Cd at 1 mg kg^{-1} wet weight and for Pb at 1.5 mg kg^{-1} wet weight (Official Journal of the European Communities, 2001). These limits represent 4 mg kg^{-1} dw for Cd and 6 mg kg^{-1} dw for Pb, if we assume the mean moisture of 75% obtained in the samples analyzed. With the use of VIS spectroscopy it is possible to determine quickly which samples have Pb and Cd contents below or above the limits. In the second step, the reference values of the samples that have concentrations close to the lower and upper limits allowed for Cd and Pb could be analyzed by the reference method, which would provide a substantial reduction in laboratory input.

Acknowledgements

This study was supported by Project MCYT AGL2005-00619, for which the authors are deeply indebted. The authors are also grateful to the CYTED 105PI0272 project for providing technical collaboration.

References

Almela, C., Algora, S., Benito, V., Clemente, M. J., Devesa, V., Súñer, M. A., et al. (2002). Heavy metal, total arsenic, and inorganic arsenic contents of algae food products. *Journal of Agricultural and Food Chemistry, 50*, 918–923.

Ball, D. F., Barber, M., & Vossen, P. G. T. (1975). The application of high resolution spark source mass spectroscopy for the determination of trace elements in mussels. *Science of the Total Environment, 4*, 193–200.

Barnes, R. J., Dhanoa, M. S., & Lister, S. J. (1989). Standard normal variate transformation and de-trending of near-infrared diffuse reflectance spectra. *Applied Spectroscopy, 43*, 772–777.

Bayne, B. (1993). Feeding physiology of bivalves: Time-dependence and compensation for changes in food availability. In R. F. Dame (Ed.), *Bivalve filter feeders in estuarine and coastal ecosystem processes, NATO ASI series G: Ecological sciences* (pp. 1–24). Heidelberg: Springer-Verlag.

Behrens Yamada, S., & Peters, E. E. (1988). Harvest management and the growth and condition of submarket-size sea mussels, *Mytilus californianus*. *Aquaculture, 74*, 293–299.

Britton, G. (1995). UV–visible spectroscopy. In G. Britton, S. Liaaen-Jensen, & H. P. Fander (Eds.), *Carotenoids* (pp. 13–62). Basel: Birkhäuser Verlag.

Concon, J. M. (1988). Inorganic and organometallic contaminants in foodstuffs. In O. R. Fennema, M. Karel, G. W. Sanderson, S. R. Tannenbaum, P. Walstra, & J. R. Whitaker (Eds.), *Food and toxicology. Part B: Contaminants and additives* (pp. 1033–1132). New York: Marcel Dekker, Inc.

Coombs, T. L., & Keller, P. J. (1981). *Mytilus* byssal threads as an environmental marker for metals. *Aquatic Toxicology, 1*, 291–300.

Dunn, B. W., Beecher, H. G., Batten, G. D., & Ciavarella, S. (2002). The potential of near infrared reflectance spectroscopy for soil analysis – A case study from the Riverine Plain of south-eastern Australia. *Australian Journal of Experimental Agriculture, 42*, 607–614.

Feo, J. C., & Aller, A. J. (2001). Speciation of mercury, methylmercury, ethylmercury and phenylmercury by Fourier transform infrared spectroscopy of whole bacterial cells. *Journal of Analytical Atomic Spectrometry, 16*, 146–151.

Font, R., Del Río-Celestino, M., Vélez, D., De Haro-Bailón, A., & Montoro, R. (2004). Visible and near-infrared spectroscopy as a technique for screening the inorganic arsenic content in the red crayfish (*Procambarus clarkii* Girard). *Analytical Chemistry, 76*, 3893–3898.

Goldberg, E. D., & Bertine, K. K. (2000). Beyond the mussel watch – new directions for monitoring marine pollution. *Science of the Total Environment, 247*, 165–174.

Goodwing, T. W., & Britton, G. (1988). Distribution and analysis of carotenoids. UV–visible spectroscopy. In T. W. Goodwing (Ed.), *Plant pigments* (pp. 61–132). London: Academic Press Ltd.

Gorinstein, S., Moncheva, S., Katrich, E., Toledo, F., Arancibia, P., Goshev, I., et al. (2003). Antioxidants in the black mussel (*Mytilus galloprovincialis*) as an indicator of Black Sea coastal pollution. *Marine Pollution Bulletin, 46*, 1317–1325.

Hren, B., Mink, J., & Balázs, L. (2002). Fourier transform infrared analysis of gas composition in low-volume light bulbs. *Analytical Chemistry, 74*, 6402–6407.

Jensen, A., & Sakshaug, E. (1970). Producer-consumer relationships in the sea. I. Preliminary studies on phytoplankton density and *Mytilus* pigmentation. *Journal of Experimental Marine Biology and Ecology, 5*, 180–186.

Martens, H., & Naes, T. (1989). Assessment, validation and choice of calibration method. In H. Martens & T. Naes (Eds.), *Multivariate calibration* (pp. 237–266). New York: John Wiley & Sons.

Official Journal of the European Communities (2001). Regulation (EC) No. 466/2001 of the European Commission.

Osborne, B. G., Fearn, T., & Hindle, P. H. (1993). Theory of near infrared spectrophotometry. In D. Browning (Ed.), *Practical NIR spectroscopy with applications in food and beverage analysis* (pp. 13–35). Harlow: Longman Scientific and Technical.

Partali, V., Tangen, K., & Liaaen-Jensen, S. (1989). Carotenoids in food chain studies – III. Resorption and metabolic transformation of carotenoids in *Mytilus edulis* (edible mussel). *Comparative Biochemistry and Physiology, 92*, 239–246.

Pérez Camacho, A., González, R., & Fuentes, J. (1991). Mussel culture in Galicia (N.W. Spain). *Aquaculture, 94*, 263–278.

Sanjuan, A., Quesada, H., Zapata, C., & Alvarez, G. (1990). On the occurrence of *Mytilus galloprovincialis* Lmk. on NW coasts of the Iberian Peninsula. *Journal of Experimental Marine Biology and Ecology, 143*, 1–14.

Shenk, J. S., & Westerhaus, M. O. (1991). Population structuring of near infrared spectra and modified partial least squares regression. *Crop Science, 31*, 1548–1555.

Shenk, J. S., & Westerhaus, M. O. (1996). Calibration the ISI way. In A. M. C. Davies & P. C. Williams (Eds.), *Near infrared spectroscopy: The future waves* (pp. 198–202). Chichester: NIR Publications.

Stump, I. G., Kearney, J., D'Auria, J. M., & Popham, J. D. (1979). Monitoring trace elements in the mussel, *Mytilus edulis* using X-ray energy spectroscopy. *Marine Pollution Bulletin, 10*, 270–274.

Wang, W.-X., & Wong, R. C. K. (2003). Combined effects of food quantity and quality on Cd, Cr, and Zn assimilation to the green mussel, *Perna viridis*. *Journal of Experimental Marine Biology and Ecology, 290*, 49–69.

Williams, P. C., & Sobering, D. C. (1996). How do we do it: A brief summary of the methods we use in developing near infrared calibrations. In A. M. C. Davies & P. C. Williams (Eds.), *Near infrared spectroscopy: The future waves* (pp. 185–188). Chichester: NIR Publications.